ISSN 1087-6596, Glass Physics and Chemistry, 2021, Vol. 47, Suppl. 1, pp. S48–S62. © Pleiades Publishing, Ltd., 2021.

Sol-Gel Synthesis and Structure of Nanocomposites Based on Tetraethoxysilane and Boron Compounds

O. A. Shilova[a, b], I. N. Tsvetkova[a], T. V. Khamova[a, *], B. Angelov[c], I. A. Drozdova[a], I. Yu. Kruchinina[a, b], and G. P. Kopitsa[a, d]

[a] *Grebenshchikov Institute of Silicate Chemistry, Russian Academy of Sciences, St. Petersburg, 199034 Russia*

[b] *St. Petersburg State Electrotechnical University "LETI," St. Petersburg, 197376 Russia*

[c] *Institute of Physics, ELI Beamlines, Dolní Břežany, 252 41 Czech Republic*

[d] *Petersburg Nuclear Physics Institute, National Research Centre "Kurchatov Institute," Gatchhina, Leningradskaya oblast, 188300 Russia*

**e-mail: tamarakhamova@gmail.com*

Received January 25, 2022; revised February 1, 2022; accepted February 8, 2022

Abstract—The properties of sol-gel synthesis of borosilicate sols, wet gels and xerogels, as well as thin nanosized films were studied. Physicochemical processes and phenomena accompanying sol-gel synthesis of borosilicate sols, gels, xerogels, and thin spin-on glass films were analyzed on the basis of reference data and our long-term experience. Particularly, the sol-gel synthesis of borosilicate materials with high boron concentration were described in detail. The morphology, mesostructures and chemical composition of sol-gel derived borosilicate composites with a high boron content (from 30 to 48 wt %, based on B_2O_3) were studied using a number of complementary research methods (optical, scanning and transmission microscopy, small-angle X-ray scattering, and FTIR spectroscopy). The effect of sol composition (concentrations of $Si(OEt)_4$ and H_3BO_3), ofthe addition of polyols (primarily glycerol), of the conditions for synthesis and of aging of target materials on their composition were studied, as well as the morphology and mesostructures of the composites.

Keywords: sol-gel synthesis, silica sol, boric acid, glycerol, spin-on glass film, mesostructured

DOI: 10.1134/S1087659621070099

INTRODUCTION

Boron compounds, primarily boric acid and boric anhydride are widely used in the synthesis of various materials, such as glasses, ceramics, organic-inorganic composites, organic compounds, as well as protective and functional coatings. In particular, boron compounds impart chemical resistance to glasses [1], reduce the synthesis temperature of glassy and ceramic materials [2] and increase the temperature and fire resistance of organic-inorganic hybrids [3, 4]. Thin borosilicate films (spin-on glass films) are used as a source of diffusion for semiconductors in microelectronics [5–7]. Boric acid is an effective catalyst for a number of chemical reactions for organic compounds production [8]. It is successfully used as a bioactive component, as a part of biocompatible and bioresorbable implants [1, 9–11], as well as a biocidal additive in anticorrosive and fungicidal protective coatings and impregnations [1, 12]. Boric acid is used as a component of the materials that absorb radioactive radiation [13].

Boron oxide is a glass-forming oxide, capable of forming a structural network of different materials and is embedded in a silica network of several widely used glassy materials obtained both by conventional methods and using sol-gel technology [14, 15]. Borosilicate glassy materials exhibit such phenomena as microliquation—phase separation into two interpenetrating phases, more or less enriched in boron compounds [14, 16–18].

Exciting effects are observed in thin spin-on glass films (~100–250 nm) obtained from sols based on hydrolyzed tetraethoxysilane $Si(OEt)_4$(TEOS) with a high boric acid content ((30–40)B_2O_3·(70–60)SiO_2 wt %, based on dry residue) [6, 7]. Patterns formed on the spin-on glass structure of borosilicate films obtained from silica sols with a high H_3BO_3concentration vary depending on H_3BO_3 and TEOS concentrations, as well as on the film deposition conditions (temperature and humidity of the ambient air) and can be identified as Turing patterns [19]. In this respect, precursors of sol-gel synthesis can be considered as morphogens, one of which is a catalyst (H_3BO_3), and another is an inhibitor ($Si(OEt)_4$). Si–O–B bond forming, in this case, is unstable at room temperature and undergoes hydrolysis followed by a recovery [15, 19]. The formation of stable Si–O–B covalent bonds commonly

takes place during the transformation of organic compounds into inorganic substances at elevated temperatures [6, 7].

Organic-inorganic glassy borosilicate materials, as well as thin films, gels, and aerogels, including those obtained by sol-gel technology at low synthesis temperatures, are commonly non-crystalline. Therefore, their structure cannot be characterized by conventional XRD techniques. For their study, small-angle X-ray scattering (SAXS) methods should be used [14, 19–22] to characterize the hierarchical aggregation structure of sol gelation products and determine the size and the type of fractal or non-fractal organization of the resulting aggregates, as well as estimate their density or surface development features.

The effect of boron compounds on the properties of organic-inorganic composites, glasses and ceramics, as well as the study of micro-liquation processes in glasses, were discussed innumerous publications [1, 5, 9, 16–18]. Significantly less attention has been paid to the study of the micro- and mesostructure of borosilicate composites obtained from sols [2, 6, 7, 19, 23]. Nevertheless, structuring and crystallization processes taking place in solutions and in melts are largely identical [24]. Thus, the results of studying the structure of borosilicate composites obtained from sols can be useful in the characterization of glassy systems, regardless of their preparation methods. It is especially interesting to study the structure of sol-gel-derived borosilicate composites with a high boron content, since these materials and films are most in-demand for practical applications, moreover they are technologically more difficult to obtain.The aim of this study was to analyze the physicochemical processes and phenomena occurring in sol-gel-derived borosilicate micro-and nanocomposites with a high boron content, based on the published data and results of our long-term research, as well as the characterization of the chemical composition, morphology, micro-, and mesostructure of sol-gel synthesis products (sols, gels, xerogels, and thin films) and studying of the effects of variation of sol-gel synthesis conditions and sols aging using modern characterization techniques (optical microscopy, SEM, TEM, SAXS, FT-IR).

ANALYSIS OF CHEMICAL PROCESSES AND PHENOMENA OF BOROSILICATE SOLS SYNTHESIS AND IN THE RESULTING COMPOSITES

Sol-gel synthesis of silica sols, including those containing organic and inorganic modifiers and dopants, is most commonly performed in a water-alcohol medium based on alkoxy compounds in the presence of acid or alkaline catalysts [2, 6, 7, 15]. The sol-gel method has a number of advantages, such as low operating temperature, the possibility of high homogenization of precursors due to their dissolution, and carrying out reactions in solutions. This allows the formation of organic-inorganic boron-containing hybrid materials that acquire useful properties inherent in both inorganic and organic components. At an early stage of the sol-gel synthesis, the addition of organic modifiers to the borosilicate sol allows an inorganic mesh to form around larger organic oligomer and polymer molecules, thereby regulating the structure of the hybrid composite at the molecular level. Thus, through sol-gel synthesis, new borosilicate hybrid materials can be obtained [11].

The sol-gel method offers new interesting prospects for the production of borosilicate matrices with a controlled release of boron as a biocide, for example, in the preparation of coatings to protect wood from fungi and termites [25]. Sol-gel synthesis can be an alternative to the traditional method of obtaining borosilicate and borate glasses from melts, including bioactive ones [26]. There is a growing interest in the use of bioactive glass scaffolds for bone tissue regeneration using various types of bioactive borosilicate glasses [27–29].

An effective method of influencing the chemical synthesis process to achieve a better interaction between the initial components is sono-synthesis [2, 21, 30, 31].

One of the main precursors for the sol-gel synthesis of silica sols is orthosilicic acid ethyl ester $Si(OEt)_4$–tetraethoxysilane (TEOS) [6, 7, 16, 20–22, 24]. To obtain borosilicate composites, boron compounds soluble in the dispersion medium of the sol are added to the silica sol. For this purpose, boric acid H_3BO_3 is commonly used, less often esters such as trimethyl borate $B(OMe)_3$ may also be utilized [6, 7, 15, 23, 24]. The application of organoboron compounds is used, for example, for borosilylalkyl derivatives of meta-, ortho- or para-carboranes $HCB_{10-n}(CH_2{-}CH_2SiR_3)_nCH$, where R = Cl, OC_2H_5, n = 1, 2 was reported for obtaining film-forming sols and spin-on glass films used in planar technology of microelectronics as sources of boron diffusion in semiconductor materials [32].

Boric acid is the most commonly used additive as a low-toxic, easily dosed, cheap, and readily available reagent. In addition to acting as a dopant in the sol-gel synthesis, boric acid, depending on its concentration, can play a role of both: a catalyst for TEOS hydrolysis and a reagent inhibiting the transformation of silica sol into a gel [7]. The disadvantage of boric acid application in sol-gel synthesis is its low solubility in water and simple alcohols, which are most commonly used in the synthesis of TEOS-based sols. Therefore, in order to obtain silica sols with a high boron concentration, boric acid is preliminarily dissolved in glycerol or in a mixture of glycerol with simple alcohols [2, 6, 7, 21]. The interaction of glycerol with boric acid was described in numerous researches. The donor-acceptor interaction of boric acid with glycerol results in the formation of a complex acid being much stronger than the initial acid and contains the bis-ethylene borate

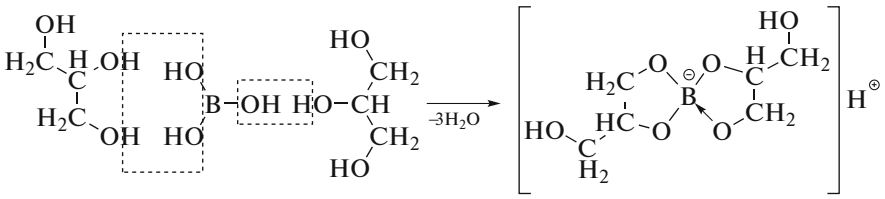

Fig. 1. The formation of a complex compound from boric acid interaction with glycerol.

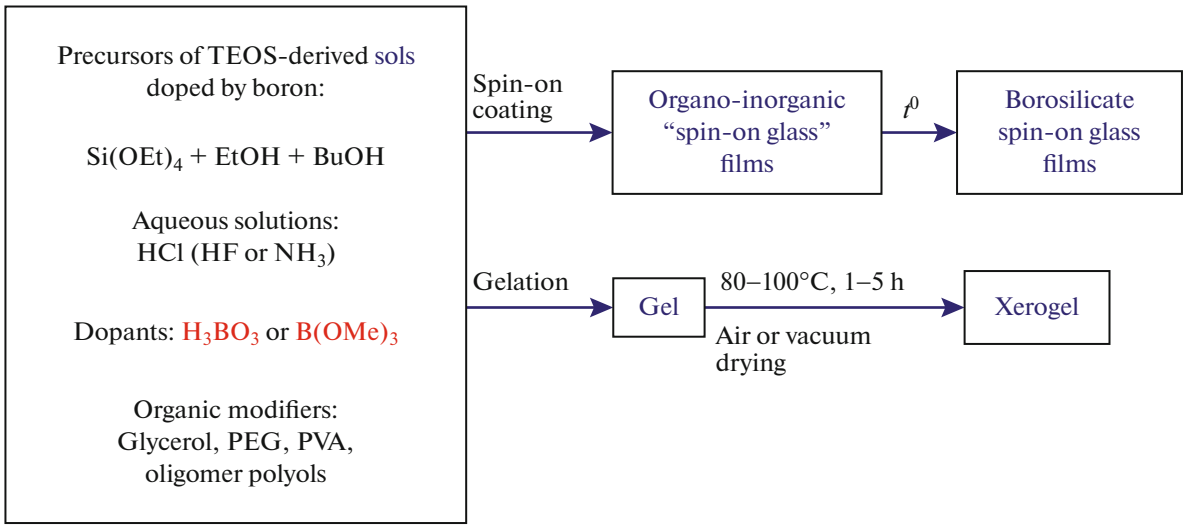

Fig. 2. General scheme of possible approaches to sol-gel synthesis of borosilicate nanocomposites.

anion (Fig. 1) [33].The composition and the properties of complex acids are determined by the concentration and the ratio between the donor and the acceptor. Complex acids are known to possess surface-active properties [34]. This is probably why boric acid improves the aggregation stability and inhibits the viscosity growth of silica sols in a water–alcohol dispersion medium.In the sol-gel synthesis of borosilicates, aqueous solutions of NH_3, HCl or HF can be used as catalysts. Based on our experience in obtaining borosilicate nanocomposites, we summarized possible approaches to the sol-gel synthesis of thin (100–300 nm) borosilicate films and xerogels, schematically shown in Fig. 2. It is often required to obtain a borosilicate nanocomposite with high boron content. In this regard, a number of difficulties may arise in the implementation of sol-gel syntheses, such as low solubility of the precursors, their high volatility, changes in the morphology and texture of the resulting materials and coatings. An example of the sol-gel synthesis of a borosilicate composite with high boron content has been described in detail in our previous study [2]. In the first series of experiments, borosilicate nanocomposites were synthesized using boric acid as a source of B_2O_3, preliminarily dissolving boric acid in glycerol to obtain sols corresponding to a mineral composition of $48B_2O_3{\cdot}52\,SiO_2$ mol % (by synthesis). In the second series of experiments, trimethyl borate $B(OCH_3)_3$(TMB) was used. This approach provided sols with higher boron concentrations based on B_2O_3 ($98B_2O_3{\cdot}2\,SiO_2$ mol %, by synthesis). An increased content of boric anhydride in the resulting xerogel promoted a decrease of the transition temperature of the organosilicon composite into the oxide state if it is necessary to obtain an inorganic borosilicate material and to enhance the fire resistance at obtaining an organic-inorganic composite [2].

A highly inert and stable Si–O–B bond, identical to bonds in borosilicate glasses, is quite difficult to obtain by sol-gel synthesis at room temperature without additional external influences. This complication is determined by a high reactivity of boron precursors (H_3BO_3, $B(OMe)_3$) towards water, causing the precipitation of boric acid instead of the formation of Si–O–B bonds [15, 19, 35]. Hydrolysis and condensation of TMB can occur according to the S_N mechanism, involving a nucleophilic attack by OH or OR groups in electrophilic trigonal boron with the corresponding release of water or alcohol [36]. It was reported that the higher is the molecular weight R of the borate esters, the slower is the rate of hydrolysis [36]. Irwin et al. [37] revealed that all these reactions proceed first through the formation of =B–O–Si≡ bonds followed by their

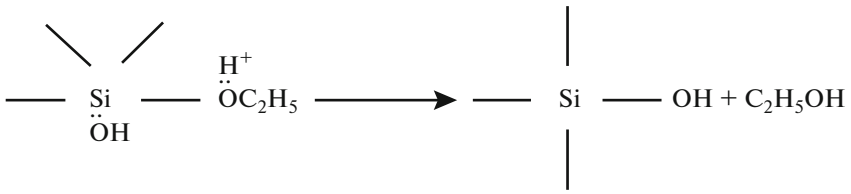

Fig. 3. Scheme of ultrasonically activated non-aqueous hydrolysis of TEOS in the presence of glycerol and boric acid.

gradual disappearance. Trialkylborates are known to react with water much faster than silicon alkoxides; particularly at room temperature they almost instantly hydrolyze into boric acid.

Since triple coordinated boron is more electrophilic than silicon, the hydrolysis of its compounds yielding boric acid proceeds faster. Si–O–B bonds are formed mainly as a result of the reaction of boric acid with silanol groups. A high alcohol content (particularly methanol, if $B(OMe)_3$ is used) accelerates the alcoholysis of borosiloxane bonds, i.e. shifts the reaction equilibrium towards the initial compounds.

In [21], an ultrasonically-assisted procedure of non-aqueous hydrolysis of $Si(OEt)_4$ in the presence of $H_3BO_3$was studied. The experiment was carried out using TEOS, boric acid and glycerol. The reagents were mixed in the molar ratio $Si(OEt)_4$: (H_3BO_3 + $CH_2OH–CHOH–CH_2OH$) = 1 : (1.8 + 6). Two portions of this composition were used in the synthesis with (no. 1) and without (no. 2) sonication (22 kHz, 20 min). Both mixtures were placed in closed containers. A week later, a transparent gel formed in vessel no 1 as the result of sonification, which turned into wet transparent xerogel granules after drying in a vacuum at 80°C. On the contrary, mixture no. 2 separated into two immiscible liquids without gelation. Thus, the TEOS hydrolysis proceeded under ultrasonication even in the absence of water and a strong acid catalyst. In this case the abstraction of OH groups from the glycerol molecule and their interaction under the influence of boric acid protons (apparently abstracted due to ultrasonic processing) formed silanol groups and released the alcohol similar to the reaction activated by an acid catalyst (Fig. 3).

Then the resulting alcohol could join the reaction with silanol groups to form latent water that in turn could undergo the sonication-induced dissociation into hydroxyls and protons subsequently reacting with TEOS.

In [11] the sol-gel method was used to obtain a composite based on borosilicate gel (BG) and polyvinyl alcohol (PVA). PVA-BG hybrid frameworks were prepared using the following sol-gel process: first, 26.7 mL of TEOS was dissolved in 80 mL of ethanol, followed by the addition of 4.3 ml of HNO_3 (1M) solution to initiate the TEOS hydrolysis reaction at 40°C, subsequently stirred for 1 h. After stirring for another 3 h, a borosilicate sol was obtained, subsequently mixed with an aqueous solution of PVA (5 wt %) previously prepared by dissolving PVA in deionized water at 90°C. The results of IR spectroscopy showed that [BO_3], [BO_4] and [SiO_4] units bonded with each other to yield a borosilicate network subsequently forming chemical bonds with PVA.

Thus, the sol-gel synthesis of borosilicates from TEOS and H_3BO_3 (or TMB) in a mixed aqueous-alcoholic medium in the presence of acidic or alkaline catalysts yielded silica sols containing boron compounds. In this case, at room temperature, the Si–O–B bond was present in a vibrational state consecutively undergoing hydrolysis and recovery [15, 19]. The formation of a stable Si–O–B bond was only possible with additional external impacts, for example by heating or prolonged stirring at an elevated temperature.

Polyhydric alcohols glycerol and PVA were successfully used in the sol-gel synthesis of borosilicates. The use of glycerol made it possible to increase the boron content in composites, as well as to carry out a sonication activated sol-gel synthesis in a non-aqueous medium. The use of PVA allowed obtaining organic-inorganic borosilicate composites with elasticity.

The use of small additives (0.7–2.0 wt %) of polyethylene glycol and branched or hyperbranched oligomers containing a few of reactive functional groups (primarily OH groups as well as urethane groups –N(R) –C(O)O–R=H, alkyl or acyl), MW = 2.000–5.000) was described in [6, 38]. It was found that the critical threshold concentration of oligomers 2 wt % lead to the destruction of the structural network in the silicon-organic composite formed in the sol [38]. The addition of oligomeric polyols modified the spin-on glass film morphology making the film surface more developed and increasing the film thickness (by 1.5–2 times) without breaking the integrity during the heat treatment [6].

So far, the processes of structural evolution of hybrid borosilicate sols during gelation at the formation and aging of gels or thin films have been studied insufficiently. We performed experimental studies of the borosilicate composites (wet and dry gels (xerogels), spin-on glass films) composition and structure obtained by the sol-gel method based on TEOS, H_3BO_3 and glycerol, depending on the concentration of boric acid and TEOS in sols. The results of these studies are described in the following sections.

Table 1. Compositions of film-forming borosilicate sols

Composition designation	Xerogel composition, wt % (by synthesis, based on dry residue)	The ratio between the initial components, vol %			
		$Si(OEt)_4$	H_3BO_3 6% solution* in EtOH	HCl 0.25 N aqueous solution	BuOH
30B-70Si_10TEOS	$30B_2O_3{\cdot}70SiO_2$	10	34	5	51
30B-70Si_20TEOS		20	68	10	2
30B-70Si_20TEOS_Gl		20	68*	10	2
40B-6i0Si_10TEOS	$40B_2O_3{\cdot}60SiO_2$	10	53	5	32
40B-60Si_10TEOS_Gl		10	53*	5	32
40B-60Si_20TEOS		20	106	10	–
40B-60Si_20TEOS_Gl		20	106*	10	–

* With the addition of 5 mL glycerol per 100 mL of the solution.

EXPERIMENTAL

Sol-gel Synthesis of Film-Forming Borosilicate Sols

Borosilicate sols based on TEOS and H_3BO_3 can be film-forming at a certain ratio of the initial components. At 10–20 vol % concentration of TEOS hydrolyzed in an acidic medium it is possible to obtain sols that do not transform into a gel for a long time. Thin borosilicate films from this medium can be applied to the surface of glass, ceramics and semiconductor materials useful in optical and electronic industries [6, 7].The objects of this study were sols with different concentration ratios between the main components (TEOS and H_3BO_3), corresponding to the mineral composition of $40B_2O_3$–$60SiO_2$ and $30B_2O_3$–$70SiO_2$ (based on dry residue) at two concentrations of TEOS (10 and 20 vol %). The sols were synthesized by acid hydrolysis of TEOS, according to a single-step procedure involving a consecutive mixing of ButOH, the pre-mixed 6% alcohol solution of H_3BO_3, 0.25 N aqueous solution of HCl, and $Si(OEt)_4$. An alcohol solution of H_3BO_3 was prepared by mixing boric acid and ethanol with the addition of glycerol at a ratio of 5 mL per 100 mL of solution. The compositions of the resulting sols are given in Table 1.

Preparation of Sol-Gel-Derived Composites

Spin-on glass films were coated by film-forming sols (see Table 1) after centrifugation at 2000 rpm using a special centrifuge in a hermetic pressure chamber, where the temperature (t) and relative humidity (φ) of the ambient air varied during the application process from +15 to +40°C and φ varied from 40 to 85%. After deposition, the films were subjected to heat treatment at 700°C.

Xerogels for small-angle X-ray scattering (SAXS) were prepared from the film-forming sols (see Table 1) by aging in air at room temperature, followed by drying in an oven at 100°C.

Borosilicate sols with the higher content of H_3BO_3 and glycerol were obtained using TEOS (20 vol %) hydrolyzed from an acidic medium in the presence of boric acid and glycerol (38 mL per 100 mL of the borosilicate sol). The molar ratio of the components in the sols was $Si(OC_2H_5)_4$: H_2O : C_2H_5OH : $C_3H_8O_3$: H_3BO_3 = 1 : 1.3 : 6 : 6 : 1.8. The weight fraction of H_3BO_3 was determined by the calculation for the target borosilicate composite of the mineral composition $48B_2O_3{\cdot}52SiO_2$ (wt %). The sols were homogenized by ultrasound (44 kHz, 10 min). The short designation for this composition was 48B-52Si_20TEOS_Gl.

Borosilicate wet gel and xerogel for FTIR were prepared from the sol 48B-52Si_20TEOS_Glafter gelation and drying in air (wet gel) and after heat treatment at 500°C, 1 h (xerogel).

For TEM we used both a freshly prepared **wet gel** and **dry gel** obtained in the course of slow aging the sol 48B-52Si_20TEOS_Gl in air for a very long time (7 years).

Characterization of the Surface Morphology and Mesostructures of the Composites

The surface morphology of thin films (spin-on glass films) was studied using an optical metallographic microscope in reflected light in a bright field. Crystallites in the films were characterized by scanning electron microscopy (SEM) in reflected electrons.Freshly prepared wet gels and dry gels aged for 7 years were examined using a transmission microscope (TEM).The mesostructures of borosilicate gels were studied by the SAXS method on the prepared xerogel samples. SAXS measurements were carried out using the Molecular Metrology SAXS System (Institute of Macromolecular Chemistry, Prague) operating in axial geometry and using a CuKα microfocus X-ray generator (λ = 0.154 nm) Osmic MicroMax 002 operating at 45 kV and 0.66 mA (30 W). The spectrometer was equipped with a gas-filled detector

with an active area of 20 cm in diameter (Gabriel design). The use of two sample positions made it possible to measure the intensity of X-ray scattering in the range of transmitted pulses $5.5 \times 10^{-2} < q < 9$ nm^{-1}, corresponding to the analysis of borosilicate composites supramolecular structure in the range of characteristic sizes R_c from 0.5 to 60 nm. All the measurements were carried out in vacuum at ambient temperature.The chemical composition of the same sols from which spin-on glass films formed, both with and without glycerin (see Table 1), as well as wet gel and xerogel obtained by the above method from sols with high content of boric acid and glycerol (48B-52Si_20-TEOS_Gl), were investigated by FTIR spectroscopy. IR spectroscopic studies were carried out in the reflected mode in the range 600–4000 cm^{-1} using an FSM 2202 IR FTIR spectrometer (Russia) and a horizontal ATR accessory attachment.

RESULTS

Macrostructure of Borosilicate 2D Composites

It should be noted that transparent homogeneous borosilicate films could be obtained from borosilicate sols with high boron content only in the case of their rapid formation. This was achieved by either spin-coating or dip-coating, i.e. application by means of a centrifuge or immersion and rapid uniform stretching of substrates from film-forming sols [6, 7, 15]. In our studies, it was found that if the concentrations of TEOS in borosilicate sols were higher than 10 vol % and H_3BO_3 were higher 30 wt % B_2O_3, it would be impossible to obtain transparent spin-on-glass films since they became opaque. Micro- and macro- separations were observed in such films using optical and scanning electron microscopes [6, 7, 19]. A typical appearance of such micrometer-scale phase separations in borosilicate films containing 30 and 40 wt % B_2O_3 (based on dry residue, according to the synthesis, see Table 1) is presented in Fig. 4. Our studies revealed that the tendency to phase separation (microliquation) strengthened both in the course of borosilicate sols aging (i.e. with the increase of their viscosity) (Figs. 4a, 4b) and in case of a change in film deposition conditions (decrease of the ambient temperature below 20°C and increase of the relative humidity above 50%). The phenomenon of micro-liquation was becoming more and more prominent. Boric acid crystals began to precipitate from one of the interpenetrating phases, apparently more enriched in boron (Fig. 4b). With a more significant decrease in the ambient air temperature during the film deposition (up to +15°C), boric acid crystals began to precipitate from the second phase, which was less enriched in boron, and crystallites in the areas more enriched in boron became more prominently crystallized (Fig. 4c). An increase of boric acid concentration in the sol (up to 40 wt % B_2O_3) further catalyzed the above-described tendency of high-doped borosilicate films to phase separation and crystallization (Figs. 5a, 5b), even despite a decrease in TEOS concentration in borosilicate sol to 10 vol %. Formation of transparent films was found to be only possible upon pre-dissolving of boric acid in ethanol with the addition of glycerol (Fig. 5c).The introduction of glycerol into borosilicate sols promoted an increase in both solubility of boric acid and solution viscosity, thereby inhibiting the evaporation of the dispersed sol medium during spin-coating. As a result, a polysiloxane gel network had time to form on the substrate surface before H_3BO_3 crystallites began to form as a result of solvent evaporation and supersaturation of the dispersion medium with boric acid [6, 7].Thus, during the formation of borosilicate 2D objects – spin-on glass films obtained from TEOS-based sols with a high H_3BO_3 content, interesting phenomena were discovered associated with micro-liquation clearly visible at the micrometer level. In this regard, it was essential to study the organization of the supramolecular structure of borosilicate nanocomposites at a mesoscale exploring the potential of small-angle X-ray scattering (SAXS) and transmission electron microscopy (TEM).

Mesostructure of Borosilicate Nanocomposites

Figures 6 and 7 represent experimental plots of X-ray scattering intensity I_s as a function of momentum transfer q in the double logarithmic scale for borosilicate nanocomposites with TEOS concentrations 10 vol % (Fig. 6) and 20 vol % (Fig. 7).

A common feature for all the studied borosilicates was the presence of two intervals of momentum transfer q values in the scattering plots with drastically different behavior of SAXS $I_s(q)$ intensity. In the range $q < q_c$ (where q_c is a crossover point corresponding to the transition from one scattering mode to another) the scattering intensity $I_s(q)$ followed a power law q^{-n} for all the considered nanocomposites. Such a power dependence is known to be observed in the case of a wide distribution of scattering inhomogeneities in the size range $R_{max} \gg R_{min}$, provided the following condition is satisfied:

$$R_{max}^{-1} \le q < R_{min}^{-1}. \quad (1)$$

In addition, a power law of scattering means that inhomogeneities mainly contributing to scattering intensity were large enough to fulfill the condition $q_{min}R \gg 1$. In [39], a more accurate practical criterion was proposed to determine the characteristic size of inhomogeneities as $q_{min}R \approx 3.5$. According to this approach, in this case $q_{min} = 5.7 \times 10^{-2}$ nm^{-1} and the corresponding characteristic size of inhomogeneities was $R \approx 61.5$ nm.

The values of the power degree n determined from the slope of the linear areas in $I_s(q)$ plots in double logarithmic scale were in the range from 4.01 to 4.16 for

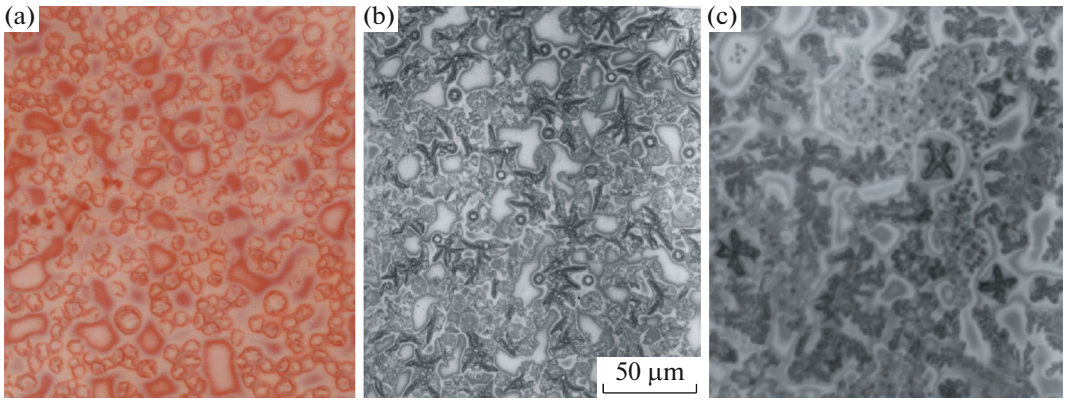

Fig. 4. Morphology of spin-on glass borosilicate films spin-coated from the 30B-70Si_20TEOS sol after their aging within 1 (a) and 3 months (b, c), under normal conditions (a, b) and at low ambient air temperature (+15°C) (c).

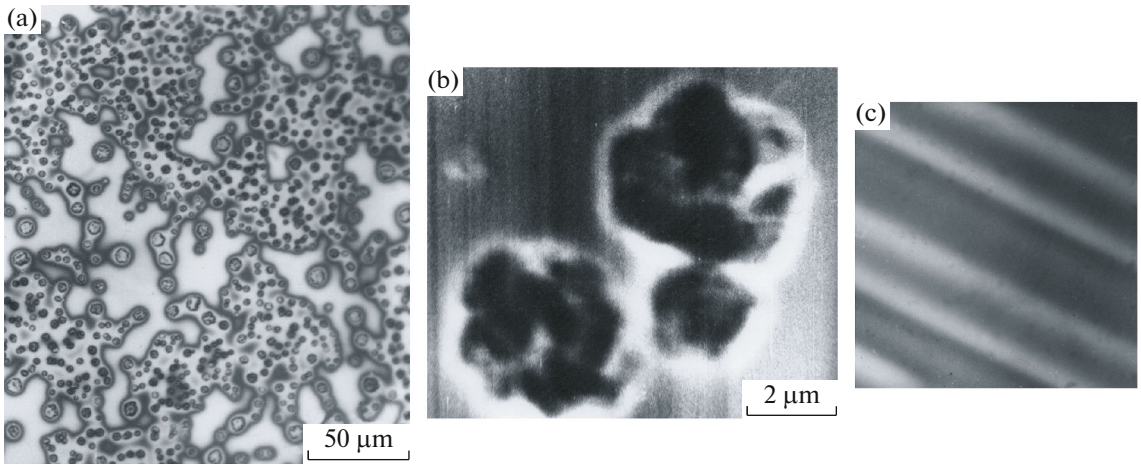

Fig. 5. Optical microscopic image of the surface of borosilicate films prepared from sols: 40B-60Si_10TEOS without glycerol (a) and 40B-60Si_10TEOS_Gl with glycerol (c). SEM images of crystallites in the film prepared from glycerol-free sol (b).

all the studied borosilicate composites, except for the sample 30B-70Si_10TEOS featuring $n = 3.74 \pm 0.02$. This power law was intrinsic to systems containing dissipating inhomogeneities with a so-called "diffuse" surface [40], for which the power degree followed the condition $n = 4 + 2\beta > 4$, where $0 \le \beta \le 1$ is the power factor characterizing the law of changes in nuclear density ρ in the surface layer of inhomogeneities. In the case of borosilicate composite 30B-70Si_10-TEOS, the scattering occurred on inhomogeneities with a developed fractal surface of the phase separation interfaces with the dimensions $D_S = 6 - n = 2.26 \pm 0.02$ [41].

In the range $q > q_c$, scattering plots for all the samples contained a broad peak with the position obviously dependent on TEOS concentration (Figs. 6 and 7). According to [44], the appearance of this peak in SAXS $I_s(q)$ plots relates to structural correlations of near-order type in the location of contrasting inhomogeneities (particles).

In this case, taking into account inter particle interactions, the behavior of SAXS intensity $I_s(q)$ is described by the following equation [42]:

$$I_s(q) = \varphi\nu(\Delta\rho^2)F(q)^2S(q), \quad (2)$$

where: $F(q)$ is the shape factor function of the scattering inhomogeneity (F) of particle (q), ν is the inhomogeneity (particle) volume, φ-volume part of scattering inhomogeneities (particles) and $\Delta\rho = \rho(r) - \rho_s$ is the contrast, i.e. the difference between the scattering amplitude densities on inhomogeneities $\rho(r)$ and in the environment ρ_s. The parameter $S(q)$ in the equation (2) is the structural factor (correlator) responsible for interparticle structural correlations. In the case of random distribution of scattering particles $S(q) = 1$, and scattering follows the equation [43]:

$$I_s(q) = G_0 \exp\left(-\frac{q^2R_g^2}{3}\right) + \frac{B_0}{\hat{q}^{n_0}} + I_{inc}, \quad (3)$$

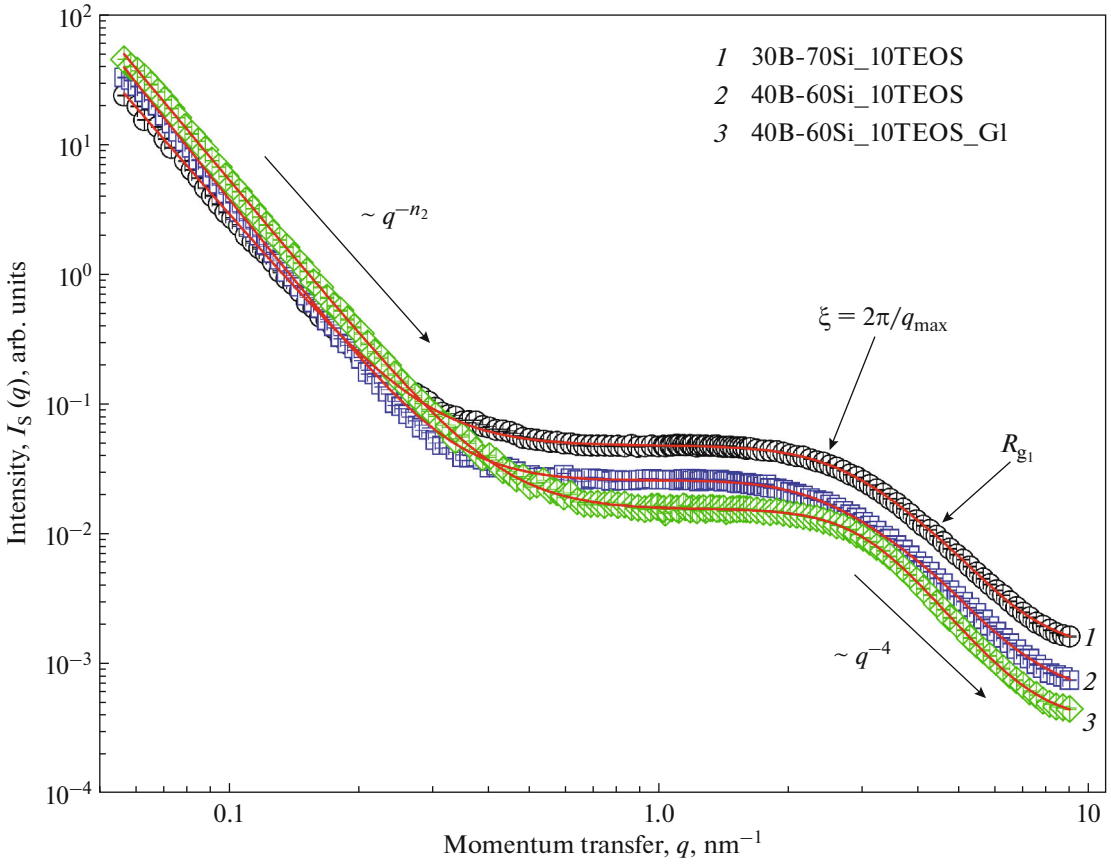

Fig. 6. SAXS intensity $I_s(q)$ plot for borosilicate nanocomposites with TEOS concentration 10 vol % (see Table 1).

where $\hat{q} = \dfrac{q}{\left[\mathrm{erf}\left(\dfrac{qR_g}{6^{1/2}}\right)\right]^3}$ is the momentum transfer q normalized to the error function erf(x); the amplitudes G_0 and B_0 are free parameters, the former (Guigner pre-factor) being directly proportional to the contrast $\Delta\rho$, and the latter (power pre-factor) depending on the local structure [44]; R_g is the gyration radius of scattering inhomogeneities, that in the case of their spherical shape relates with the intrinsic size of inhomogeneities be the expression $R_c = \sqrt{\frac{5}{3}}R_g$ [44]; parameter I_{inc} is a constant independent of q and determined by incoherent scattering on inhomogeneities of the order of wavelength of the applied CuK_α ($\lambda = 0.154$ nm) radiation.

To analyze the structural correlations, we used a semi-empirical function for $S(q)$ earlier suggested in [42, 45, 46] and reliably describing flowing spherical correlations of colloid particles in terms of the correlation radius ξ and packaging factor κ in our studies [47–49].

$$S(q) = \frac{1}{(1 + \kappa\theta)}, \quad (4)$$

where: θ is the shape factor for structural spherical correlations in the scale ξ:

$$\theta = 3\frac{(\sin(q\xi) - q\xi\cos(q\xi))}{q\xi^3}. \quad (5)$$

The packaging factor κ characterizes the degree of structural correlations ($0 < \kappa < 5.92$, for weak correlations $\kappa < 3$). The correlation radius $\xi = 2\pi/q_{max}$ (where q_{max} is the position of the maximum in the plot for $d\Sigma(q)/d\Omega$) corresponds to the average distance between the centers of inhomogeneities.

Thus, the scattering pattern observed for the studied borosilicate composites was typical for systems involving two types of inhomogeneities strongly differing in the characteristic size R_c, with smaller inhomogeneities being structured according to the near-order type. In accordance with these features, we analyzed the scattering plots $I_s(q)$ in the entire range of momentum transfer values q using a unified exponential-power approximation for two-level structures, taking into account the presence of structural correlations of near-order type for the smaller structural level [42]:

$$I_s(q) = \frac{B}{q^n} + \left(G_0 \exp\left(-\frac{q^2R_{go}^2}{3}\right) + \frac{B_0}{\hat{q}^{no}}\right)S(q) + I_{inc}, \quad (6)$$

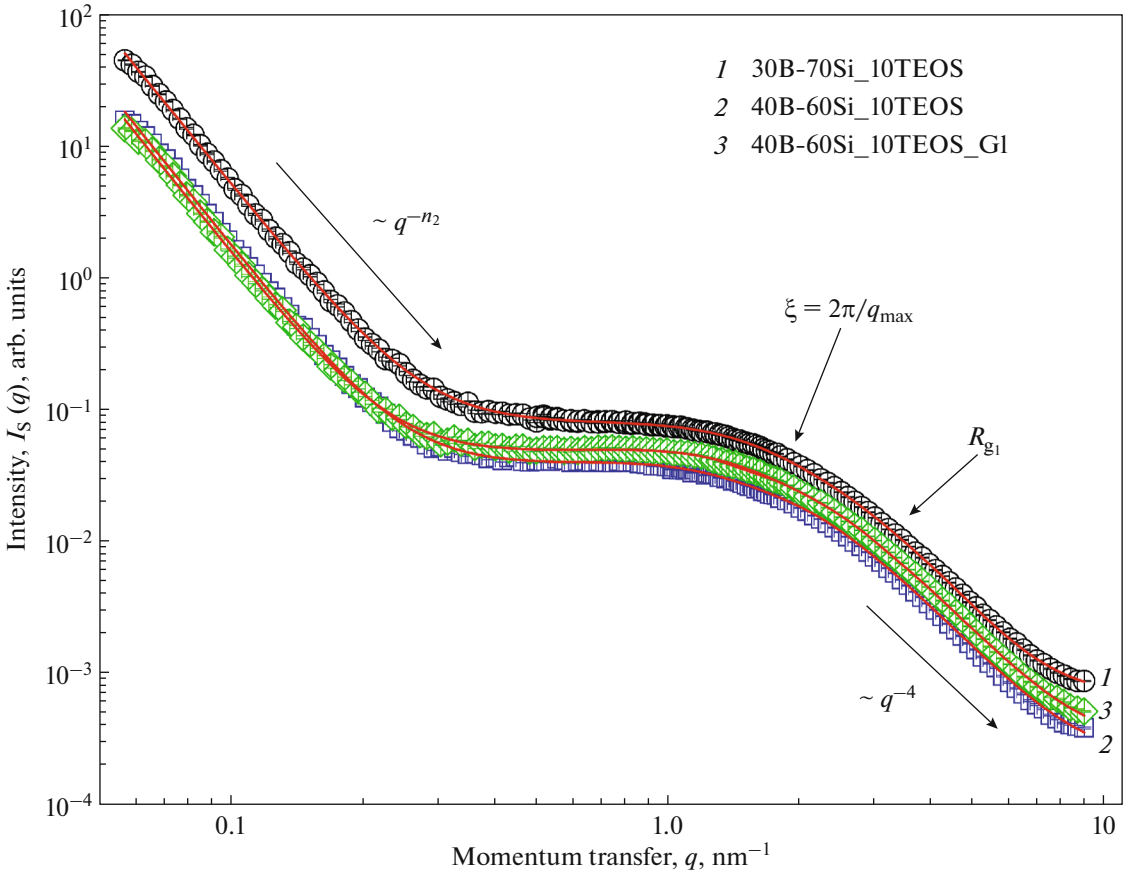

Fig. 7. SAXS intensity $I_S(q)$ plot for borosilicate nanocomposites with TEOS concentration 20 vol % (see Table 1).

To obtain the final results, the expression (6) was applied to get her with the installation resolution function and treated according to the least squares method. As a result of fitting, the power degree n_0 was found to be equal to 4. The data of performed processing are presented in Figs. 6 and 7, as well as in Table 2.

The data summarized in Table 2 show that in the scale level from 1 to 100 nm all the synthesized borosilicate xerogels were non-fractal systems with a two-layer hierarchical mesostructured organization. The first structural level involved primary siloxane particles with the diameter $D_c \approx 1.2–1.7$ nm. On the second structural level they formed large scale ($D > 120$ nm) aggregates possessing a "diffuse" surface, with the exception of the sample 30B-70Si_10TEOS. In addition, weak structural correlations of the near-order type existed between primary siloxane particles (which was common for glassy state of matter [14]) with the average distance between the particle centers $\xi \approx 1.9–5.2$ nm and the packaging factor $\kappa \approx 0.23–0.72$. It is also clear that both the size of the primary siloxane particles and the radius of structural correlations ξ in borosilicate xerogels grew with the increase of TEOS concentration. In turn, the packaging factor κ, determining the degree of correlations between particles, decreased with increasing TEOS concentration. At the same time, the presence of a modifying additive glycerol lead to an increase in the parameter κ for samples with the same TEOS concentration.

SAXS data characterizing the xerogels structure on the level from nanometers to tens of nanometers were in good agreement with TEM results indicating the gel (xerogel) structure on the scale from tens to hundreds of nanometers. Figure 8a clearly shows that the mesostructure of the wet gel was quite uniform but included individual particles and agglomerates, although no boric acid crystallites were observed. Due to a very slow (for 7 years) aging, gradual evaporation of the solvent and absence of external influences the gel structure was almost undeteriorated (Fig. 8b). However, agglomerates (apparently, SiO_2 nanoparticles) became more dense and prominent in the TEM images. A larger magnification allowed the visualization of nanoparticles composing these agglomerates (Fig. 8d). In some areas, well faceted boric acid crystals formed over time were observed (Fig. 8c).

The aged dry gel can be considered possessing a diffuse type of structure, i.e. featuring the gradient structure, as clearly observed in Fig. 8e. Interestingly, the analysis of SAXS data on the change of nuclear

Table 2. Mesostructure parameters of borosilicate nanocomposites, SAXS data

Designation (see Table 1)	Parameters			
	n	$D_c = 2R_c$, nm	ξ, nm	κ
30B-70Si_10TEOS	3.82 ± 0.02	1.16 ± 0.05	2.2 ± 0.2	0.37 ± 0.01
40B-60Si_10TEOS	4.16 ± 0.02	1.20 ± 0.05	2.6 ± 0.1	0.35 ± 0.03
40B-60Si_10TEOS_Gl	4.01 ± 0.02	1.22 ± 0.05	1.9 ± 0.1	0.72 ± 0.05
30B-70Si_20TEOS	4.07 ± 0.02	1.72 ± 0.06	4.1 ± 0.2	0.23 ± 0.02
40B-60Si_20TEOS	4.16 ± 0.02	1.68 ± 0.06	5.2 ± 0.2	0.25 ± 0.03
40B-60Si_20TEOS_Gl	4.15 ± 0.02	1.68 ± 0.06	4.6 ± 0.2	0.33 ± 0.02

n—power degree, D_c—diameter of spherical inhomogeneities of the 1st structural level, ξ—structural correlation radius,κ—packaging factor.

density in the surface layer of inhomogeneities also allowed us to reveal a diffuse structure for freshly prepared xerogels of all the compositions, except for 30B-70Si_10TEOS (with the lowest content of both TEOS and H_3BO_3).

CHEMICAL INTERACTIONS IN SOL-GEL-DERIVED BOROSILICATE NANOCOMPOSITES

For a better understanding of the physicochemical processes occurring in sols based on TEOS and H_3BO_3, an FTIR spectral analysis of the sols, the properties of which were described above, was carried out, as well as the wet gel and xerogel obtained from the sol with the highest boric acid and glycerol content. The results are shown in Fig. 9.

The spectra of the film-forming sols (Fig. 9, *1*–*3*), contain the following characteristic bands: bands around 640, 670 cm^{-1} are assigned to a B–O–Si bending vibration; bands in the range of 840–650 cm^{-1} correspond to Si–O–Si symmetric stretching vibrations; bands around 970–860 cm^{-1} are attributed to stretching vibrations of Si–OH and B–O–Si; bands around 1220–1020 cm^{-1} are attributed to Si–O–Si asymmetric stretching vibrations; bands around 1637–1650 cm^{-1} are assigned to adsorption due to water; the complex set of bands between 1290 and 1500 cm^{-1} are

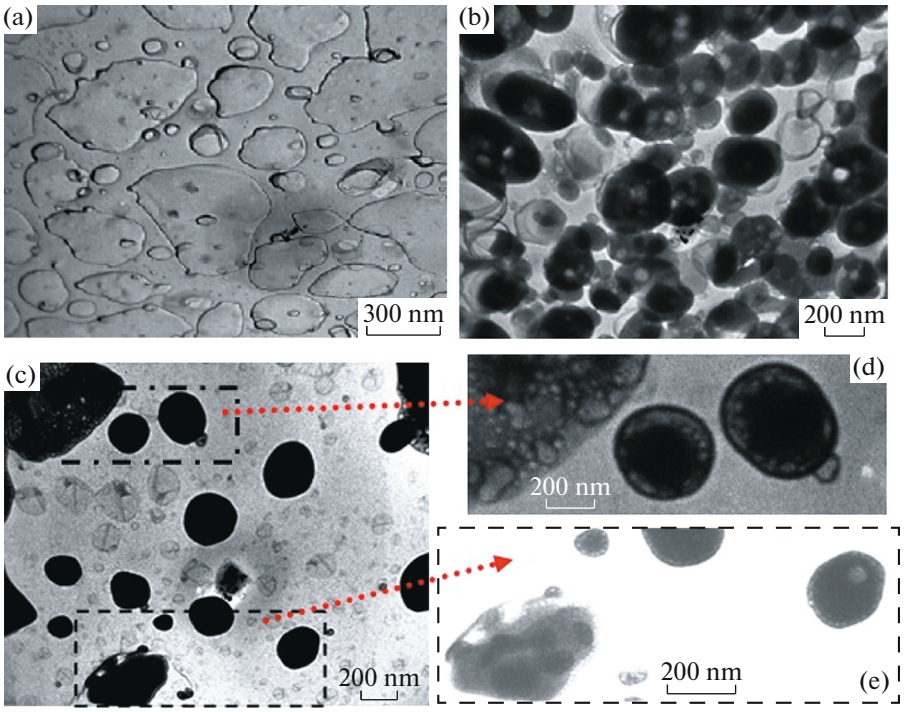

Fig. 8. TEM images of freshly prepared wet borosilicate gel (a) and slowly (within 7 years) dry gel (b, c). Inserts (d, e) illustrate fragments of the image (c) with a higher magnification.

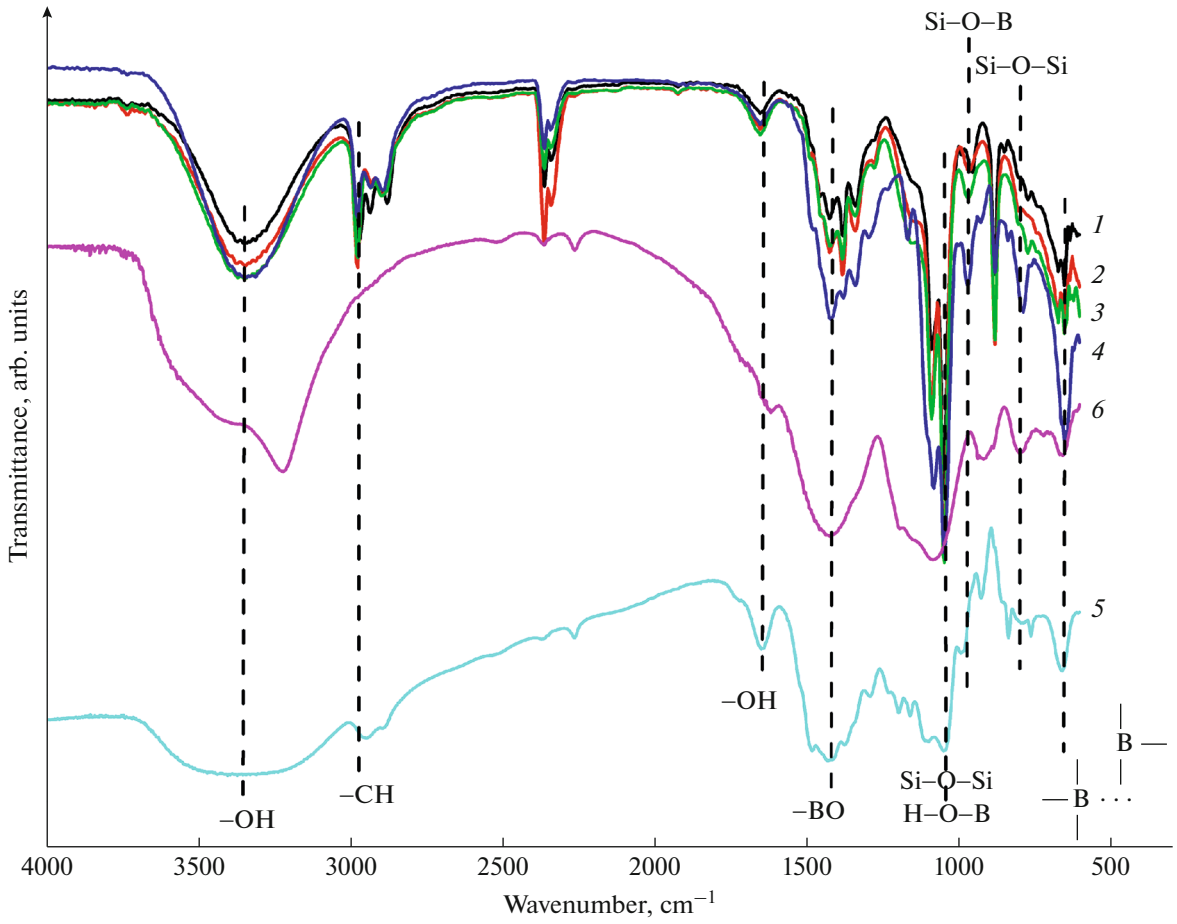

Fig. 9. FTIR spectra of TEOS-derived borosilicate sols: (*1*) 40B-60Si_10TEOS; (*2*) 40B-60Si_20TEOS; (*3*) 40B-60Si_20-TEO_Gl; (*4*) 48B-52Si_20TEOS_Gl; (*5*) wet gel and (*6*) xerogel (500°C, 2 h) prepared from sol. no. 4 (48B-52Si_20TEOS_Gl).

assigned to B–O stretching vibrations in various boron environments and to C–H deformation vibration of the alkyl groups [50–55]. Thus, for borosilicate nanocomposites prepared on the basis of TEOS and boric acid, the formation of siloxane bonds was typical even at the stage of the sol (Fig. 9). It is difficult to say precisely about the formation of stable Si–O–B chemical bonds in sols, because bands around 970–860 cm^{-1} are attributed to both Si–OH and B–O–Si. The instability of B–O–Si bonds was indirectly confirmed by the fact that all four sols contained bands characteristic of boric acid.

In the given spectra of all studied sols (Fig. 9, spectra *1*–*4*), stretching vibrations of various hydroxyl groups were manifested to a varying degree: Si–OH groups (3000–3500 cm^{-1}), SiO–H (3400 cm^{-1}), asymmetric modes Si–O–Si (1089 cm^{-1}) and BO (1432 cm^{-1}).

The addition of glycerol to borosilicate sols (Fig. 9, spectra *3*, *4*) markedly increased the absorption band at 800 cm^{-1} associated with the Si–O–H bending and indicating the presence of [SiO_4] units [11]. This may indicate the release of water as a result of the interaction of H_3BO_3 and glycerol (see Fig. 1), which promoted a more complete hydrolysis of TEOS and polycondensation of hydrolysis products with the formation of Si–O–Si bonds and, thus, an increase in the intensity of the 1048 cm^{-1}.

The broad absorption band 3100–3600 cm^{-1} (Fig. 9, spectrum *4*), characteristic of a sol with a higher content of both boric acid and glycerol, due to stretching vibrations of hydroxyl groups O–H, underwent significant changes after the transition of the sol to wet gel (Fig. 9, spectrum *5*) and then into a xerogel (Fig. 9, spectrum *6*). The band became wider, and the intensity increased due to an increase in the number of hydrogroups and water, formed as a result of chemical reactions and synergism.

The FTIR spectrum of the gel, dried in air, the heat treatment of which was not carried out (Fig. 9, spectrum *5*), has broader absorption bands at 3450–2940 and 1648 cm^{-1} than for the sol from which it was obtained. The shape of the bands of stretching and bending vibrations of water in these regions indicates that it was represented in the form of hydroxyl OH

groups, which were a structurally bound component in siloxanes.

Heat treatment (500°C, 1 h) (Fig. 9, spectrum *6*) lead to the removal of residual solvents, primarily glycerol, as evidenced by the disappearance of the absorption band in the frequency range of stretching vibrations of C–H bonds at 2950 cm^{-1}. However, a high absorption intensity remained, corresponding to the vibrations of the H–OH and Si–OH bonds. Sufficiently wide bands in the range of 1050–1150 cm^{-1}, characteristic of Si–O–Si, are most likely superimposed on absorption bands in the region of bending vibrations B–O–H.

The absorption band at 930 cm^{-1} is absent in sol (Fig. 9, spectrum *4*) due to hydrolysis of the Si–OB bond, but is observed in dry gel (Fig. 9, spectrum *5*) and xerogel heat treated at 500°C (Fig. 9, spectrum *6*), when the removal of water from the gel allowed the formation of borosiloxane bonds without them due to hydrolysis.

The obtained FTIR spectra also showed a broad absorption band in the high-frequency region of the spectrum at 660 cm^{-1}. This band indicates the presence of boron in triple coordination [BO_3] [11, 56] and a hybrid interpolymer complex [BO_4] (Fig. 1) [13].

BOROSILICATE NANOCOMPOSITES APPLICATIONS

Spin-on glass films are used in semiconductor technology as planarization and gap-fill, low relative permittivity (insulating layers), masking and barrier layers, passivation coatings, bonding layers, sacrificial and etch selectivity films, anti-reflective coatings, catalytic layers, and also as sources of diffusion into semiconductor materials for manufacturing integrated circuits and various electronic devices—gas sensors, MOS capacitors, etc. [57–61]. During heat treatment, a dopant diffuses from the spin-on glass films into silicon. This process stands out by its technological simplicity, the ability to regulate the type of impurity and its amount. It is used in the planar technology of microelectronics for creating modules of silicon solar cells, as well as in the technological processes of manufacturing integrated circuits and other semiconductor devices, where it is necessary to form pn junctions and highly doped regions [7, 61, 62]. In the latter case, it is important to obtain highly doped films with a homogeneous structure and surface morphology, so that diffusion structures with the required degree of doping can be reproducibly obtained in a short time of heat treatment. It is interesting to note that the structure of films—sources of diffusion affects the characteristics of the obtained diffusion structures. Our studies have shown that when borosilicate films with a heterogeneous structure were used as sources of diffusion, where there were very small areas of phase separation and crystallization (less than 1 μm), a smaller amount of impurities would penetrate into the silicon lattice and the diffusion front spread to a shallower depth than when using films with a homogeneous structure [7]. Perhaps this effect was associated either with a more intense evaporation of boron from heterogeneous films during heat treatment, or with the fact that the diffusion process occurred more intensively from homogeneous, uniformly boron-doped glassy regions.

Borosilicate sol-gel-derived composites obtained by us, incl. in combination with organic and organosilicon modifiers (glycerin, polysiloxanes, etc.) can be used as biocidal impregnations to protect wood from biodegradants and prevent its biodegradation [12, 25].

Heat treatment (500°C, 1 h) (Fig. 9, spectrum *6*) lead to the removal of residual solvents, primarily glycerol, as evidenced by the disappearance of the absorption band in the frequency range of stretching vibrations of C–H bonds at 2950 cm^{-1}. However, a high absorption intensity remained, corresponding to the vibrations of the H–OH and Si–OH bonds. Sufficiently wide bands in the range of 1050–1150 cm^{-1}, characteristic of Si–O–Si, are most likely superimposed on absorption bands in the region of bending vibrations B–O–H.

CONCLUSIONS

Glycerol plays an important role in the sol-gel synthesis of TEOS-derived borosilicate sols, especially in the cases when obtaining thin films and gels with high boric acid content (0.6–1.8 mol H_3BO_3/1 mol $Si(OEt)_4$) is required. The interaction of glycerol with boric acid yielding a stronger complex acid provided a possibility for obtaining borosilicate sols and nanocomposites based on it (spin-on glass films, gels, xerogels) with high boron concentration (up to 30–48 wt % B_2O_3 based on the dry residue according to the synthesis), preventing from micrometer-scale microphase separation (liquation) intrinsic to borosilicate systems.

According to SAXS and TEM results, borosilicate nanocomposites are non-fractal systems with a three-level hierarchical organization of mesostructure. The first structural level involves primary siloxane particles with the diameter $D_c \approx 1.2–1.7$ nm, forming aggregates with characteristic dimensions ≈150–200 nm on the second structural level and further aggregating into larger agglomerates on the third structural level. For both primary nanoparticles in the structure of borosilicate nanocomposites and long-forming aggregates a diffuse-gradient surface structure was observed possibly due to boric acid migration to the surface.

Weak structural correlations of the near-order type were revealed between primary siloxane particles with the average distance between the particle centers $\xi \approx 1.9–5.2$ nm and the packaging factor $\kappa \approx 0.23–0.72$. The size of the primary siloxane particles and radius of

structural correlations ξ in borosilicate xerogels grew with the increase of TEOS concentration. The addition of glycerol to TEOS-derived silica sols (4–5 g per 100 mL of sol) resulted in a 1.5–2-fold increase of the packaging factor *κ*that can indirectly characterize the degree of polysiloxane structural network ordering in borosilicate nanocomposites. Based on these results, glycerol and many other polyols can be considered as template agents for the sol-gel synthesis of borosilicates.

For borosilicate nanocomposites obtained on the basis of TEOS and boric acid, the formation of siloxane bonds was characteristic already at the stage of the sol. The addition of glycerin to borosilicate sols promoted the formation of $[SiO_4]$ tetrahedra—units of the structural polysiloxane network (mesh).

Stable chemical bonds B–O–Si did not appear in sols. The instability of the B–O–Si bonds was indirectly confirmed by the fact that all sols, regardless of the concentration of TEOS, H_3BO_3, the presence or absence of glycerol, contained bands characteristic of boric acid. However, with the removal of free water, both in the wet gel and in the xerogel heat treated at 500°C, stable B–O–Si bonds formed. Both for sols and gels, including subjected to heat treatment, the presence of boron compounds in triple coordination $[BO_3]$ and a hybrid interpolymer complex $[BO_4]$ was characteristic. The presence of structurally bound water in gels and xerogels remained even after heat treatment at 500°C.

In the course of aging in both borosilicate sols and gels underwent gradually strengthening processes of SiO_2 nanoparticles aggregation, resulting in the formation of the structural networkof nanocomposites with precipitation of boric acid crystals. The increase of TEOS concentration from 10 to 20 vol % promoted the intensification of these processes.

CONFLICT OF INTEREST

The authors declare that they have no conflicts of interest.

REFERENCES

1. Balestriere, M.A., Schuhladen, K., Herrera Seitz, K., Boccaccini, A.R., Cere, S.M., and Ballarre, J., Sol-gel coatings incorporating borosilicate bioactive glass enhance anti corrosive and surface performance of stainless steel implants, *J. Electroanal. Chem.*, 2020, vol. 876, 114735.
2. Tsvetkova, I.N., Shilova, O.A., Shilov, V.V., Shaulov, A.Yu., Gomza, Yu.P., and Khashkovskii, S.V., Sol-gel synthesis and investigation of hybrid organic-inorganic borosilicate nanocomposites, *Glass Phys. Chem.*, 2006, vol. 32, no. 2, pp. 218–227.
3. Nechvolodova, E.M., Sakovich, R.A., Grachev, A.V., Vladimirov, L.V., Shashkin, D.P., Tkachenko, L.A., Shaulov, A.Yu., and Berlin, A.A., Hybrid complex polymers of boron and imidazole hydroxide, *Russ. J. Phys. Chem. B*, 2017, vol. 11, no. 5, pp. 839–845.
4. Stegno, V., Zuev, K.V., Grachev, A.V., Lalayan, V.M., Patlazhan, S.A., Shaulov, A.Yu., and Berlin, A.A., Features of the melt flow of polyethylene and boron oxide oligomer blends, *Polymer Sci., Ser. A*, 2014, vol. 56, no. 2, pp. 169–172.
5. McFarland, B. and Opila, E.J., Sol-gel derived borosilicate glasses and thin film coatings on SiC substrate: Boron loss and carbon retention due to processing and heat treatment, *J. Non-Cryst. Solids*, 2016, vol. 449, pp. 59–69.
6. Shilova, O.A., Synthesis and structure features of composite silicate and hybrid TEOS-derived thin films doped by inorganic and organic additives, *J. Sol-Gel Sci. Technol.*, 2013, vol. 68, pp. 387–410.
7. Shilova, O.A., Spin-on glass films for semiconductor technology, *Surf. Coat. Technol., B*, 2003, vol. 86, no. 3, pp. 195–202.
8. Rammohan, P., Boric acid in organic synthesis: Scope and recent developments, *Arkivoc*, 2018, Part I, pp. 346–371.
9. Oliver, J.-A.N., Su, Y., Lu, X., Kuo, P.-H., Du, J., and Zhu, D., Bioactive glass coatings on metallic implants for biomedical applications, *Bioactive Mater.*, 2019, vol. 4, pp. 261–270.
10. Peddi, L., Brow, R.K., and Brown, R.F., Bioactive borate glass coatings for titanium alloys, *J. Mater. Sci.: Mater. Med.*, 2008, vol. 19, pp. 3145–3152.
11. Pang, L., Shen, Y., Hu, H., Zeng, X., Huang, W., Gao, H., Wang, H., and Wang, D., Chemically and physically cross-linked polyvinyl alcohol-borosilicate gel hybrid scaffolds for bone regeneration, *Mater. Sci. Eng. C*, 2019, vol. 105, 110076.
12. Tsvetkova, I.N., Krasil'nikova, L.N., Khoroshavina, Y.V., Galushko, A.S., Frantsuzova, Yu.V., Kychkin, A.K., and Shilova, O.A., Sol-gel preparation of protective and decorative coatings on wood, *Sol-Gel Sci. Technol.*, 2019, vol. 92, pp. 474–483.
13. Prosanov, I.Yu., Abdulrahman, S.T., Thomas, S., Bulina, N.V., and Gerasimov, K.B., Complex of polyvinyl alcohol with boric acid: Structure and use, *Mater. Today Commun.*, 2018, vol. 14, pp. 77–81.
14. Appen, A.A., *Khimiya stekla* (Glass Chemistry), Leningrad: Khimiya, 1974, 2nd ed.
15. Brinker, C.J. and Scherer, G.W., *Sol-Gel Science: The Physics and Chemistry of Sol-Gel Processing*, San Diego: Academic, 1990.
16. Toropov, N.A., Barzakovskii, V.P., Lapin, V.V., and Kurtseva, N.N., *Diagrammy sostoyaniya silikatnykh sistem*, *Spravochnik* (Handbook on Phase Diagrams for Silicate Systems: Binary Bystems), 2nd ed., Leningrad: Nauka, 1985.
17. Antropova, T.V., Kalinina, S.V., Kostyreva, T.G., Drozdova, I.A., and Anfimova, I.N., Peculiarities of the fabrication process and the structure of porous membranes based on two phase fluorine and phosphorus containing sodium borosilicate glasses, *Glass. Phys. Chem.*, 2015, vol. 41, pp. 14–25.
18. Konon, M., Stolyar, S., Polyakova, I., Drozdova, I., Semrnova, E., and Antropova, T., Phase separated and porous glasses in the $Na_2O–B_2O–SiO_2–Fe_2O_3$ glass

forming system, *Phys. Chem. Glasses: Eur. J. Glass Sci. Technol., Part B*, 2019, vol. 60, no. 3, pp. 115–124.

19. Shilova, O.A., Fractals, morphogenesis and triply periodic minimal surfaces in sol-gel-derived thin films, *J. Sol-Gel Sci. Technol.*, 2020, vol. 95, pp. 599–608.
20. Tsvetkova, I.N., Shilova, O.A., Voronkov, M.G., Gomza, Yu.P., and Sukhoy, K.M., Sol-gel synthesis and investigation of proton-conducting hybrid organic-inorganic silicophosphate materials, *Glass. Phys. Chem.*, 2008, vol. 34, pp. 68–76.
21. Sukhyy, K.M., Gomza, Yu.P., Belyanovskaya, E.A., Klepko, V.V., Shilova, O.A., and Sukhyy, M.P., Resistive humidity sensors based on proton-conducting organic-inorganic silicophosphates doped by polyionenes, *J. Sol-Gel Sci. Technol.*, 2015, vol. 74, pp. 472–481.
22. Baranchikov, A.E., Kopitsa, G.P., Yorov, K.E., Sipyagina, N.A., Lermontov, S.A., Pavlova, A.A., Kottsov, S.Yu., Garamus, V.M., Ryukhtin, V., and Ivanov, V.K., SiO_2–TiO_2 binary aerogels: A small-angle scattering study, *Russ. J. Inorg. Chem.*, 2021, vol. 66, pp. 874–882.
23. Tsvetkova, I.N., Shilova, O.A., Drozdova, I.A., and Gomza, Yu.P., Study of the fractal structure of hybrid phosphorosilicate and borosilicate materials obtained by sol-gel method, *Perspekt. Mater.*, 2011, no. S13, pp. 888–895.
24. Bokii, G.B., *Kristallokhimiya* (Crystal Chemistry), Leningrad: Nauka, 1971.
25. Shilova, O.A., Tsvetkova, I.N., Vlasov, D.Yu., Ryabusheva, Yu.V., Sokolov, G.S., Kychkin, A.K., Nguyên, C.V., and Khoroshavina, Yu.V., in *Microbiologically Induced Deterioration and Environmentally Friendly Protection of Wood Products*, Hafiz, M.N., Bilal, I.M., Nguyen, T.A., and Yasin, G., Eds., Amsterdam: Elsevier, 2022, Chap. 13, pp. 283–321.
26. Lepry, W.C. and Nazhat, S.N., Highly bioactive sol-gel-derived borate glasses, *Chem. Mater.*, 2015, vol. 27, no. 13, pp. 4821–4831.
27. Qi, X., Wang, H., Zhang, Y., Pang, L., Xiao, W., and Jia, W., Mesoporous bioactive glass-coated 3D printed borosilicate bioactive glass scaffolds for improving repair of boned effects, *Int. J. Biol. Sci.*, 2018, vol. 14, no. 4, pp. 471–484.
28. Fu, Q., Rahaman, M.N., Bal, B.S., Bonewald, L.F., Kuroki, K., and Brown, R.F., Silicate, borosilicate, and borate bioactive glass scaffolds with controllable degradation rate for bone tissue engineering applications. II. In vitro and in vivo biological evaluation, *J. Biomed. Mater. Res. A*, 2010, vol. 95, no. 1, pp. 172–179.
29. Huang, W.H., Rahaman, M.N., Day, D.E., and Li, Y.D., Mechanisms for converting bioactive silicate, borate, and borosilicate glasses to hydroxyapatite in dilute phosphate solution, *Phys. Chem. Glasses: Eur. J. Glass Sci. Technol.*, *Part B*, 2006, vol. 47, pp. 647–658.
30. Zinatloo-Ajabshir, S., Baladi, M., and Salavati-Niasari, M., Sono-synthesis of $MnWO_4$ ceramic nanomaterials as highly efficient photocatalysts for the decomposition of toxic pollutants, *Ceram. Int.*, 2021, vol. 47, no. 21, pp. 30178–30187.
31. Zinatloo-Ajabshir, S., Heidari-Asil, S.A., Salavati-Niasari, M., and Salavati-Niasari, M., Recyclable magnetic $ZnCo_2O_4$-based ceramic nanostructure materials fabricated by simple sonochemical route for effective sunlight-driven photocatalytic degradation of organic pollution, *Ceram. Int.*, 2021, vol. 47, no. 7, pp. 8959–8972.
32. Gribov, B.G., Zinoviev, K.V., Bogdanova, L.N., Kozyrkin, B.I., Zvezdochkin, A.R., Grigos, V.I., Pechurina, S.Ya., and Mironov, V.F., Method of producing a film-forming solution, USSR Author's Certificate no. 493488, *Byull. Izobret.*, 1975, no. 44.
33. Shvarts, E.M., Ignash, R.T., and Belousova, R.G., Reactions of polyols with boric acid and sodium monoborate, *Russ. J. Gen. Chem.*, 2005, vol. 75, pp. 1687–1692.
34. Kuvshinov, V.A., Altunina, L.K., Stasieva, L.A., and Kuvshinov, I.V., Acidity study of donor-acceptor complexes of boric acid with polyols for oil displacing compositions, *J. Sib. Fed. Univ. Chem.*, 2019, vol. 12, no. 3, pp. 364–373.
35. Parashar, V.K., Orhan, J.-B., Sayah, A., Cantoni, M., and Gijs, M.A.M., Borosilicate nanoparticles prepared by exothermic phase separation, *Nat. Nanotechnol.*, 2008, vol. 3, pp. 589–594.
36. Cai, L., Lim, H., Fitzkee, N.C., Cosovic, B., and Jeremic, D., Feasibility of manufacturing strand-based wood composite treated with β-cyclodextrin-boric acid for fungal decay resistance, *Polymers*, 2020, vol. 12, no. 2, 274.
37. Irwin, A.D., Holmgren, J.S., Zerda, T.W., and Jonas, J., Spectroscopic investigations of borosiloxane bond formation in the sol-gel process, *J. Non-Cryst. Solids*, 1987, vol. 89, pp. 191–205.
38. Smirnova, I.V., Movchan, T.G., and Shilova, O.A., Specific features of structuring of film-forming silica sols in the presence of boric acid and four-arm polyol with hyperbranched structure, *Russ. J. Appl. Chem.*, 2010, vol. 83, pp. 2128–2134.
39. Bale, H.D. and Schmidt, P.W., Small-angle X-ray-scattering investigation of submicroscopic porosity with fractal properties, *Phys. Rev. Lett.*, 1984, vol. 52, p. 596.
40. Schmidt, P.W., Avnir, D., Levy, D., Hohr, A., Steiner, M., and Roll, A., Small-angle X-ray scattering from the surfaces of reversed-phase silicas: Power-law scattering exponents of magnitudes greater than four, *J. Chem. Phys.*, 1991, vol. 94, pp. 1474–1479.
41. Teixeira, J., in *Experimental Methods for Studying Fractal Aggregates*, Stanley, H.E. and Ostrowsky, N., Eds., Dordrecht: Springer, 1986.
42. Beaucage, G. and Schaefer, D.W., Structural studies of complex-systems using small-angle scattering - a unified Guinier power-law approach, *J. Non-Cryst. Solids*, 1994, vols. 172–174, no. 2, pp. 797–805.
43. Beaucage, G., Approximations leading to a unified exponential/power-law approach to small-angle scattering, *J. Appl. Crystallogr.*, 1995, vol. 28, pp. 717–728.
44. Schmidt, P.W., *Some Fundamental Concepts and Techniques Useful in Small-Angle Scattering Studies of Disordered Solids*, Dordrecht: Kluwer, 1995.
45. Guinier, A. and Fournet, G., *Small-Angle Scattering of X-Rays*, New York: Wiley, 1955.
46. Roe, R.J., *Methods of X-Ray and Neutron Scattering in Polymer Science*, New York: Oxford Univ. Press, 2000.
47. Ivanov, V.K., Kopitsa, G.P., Baranchikov, A.E., Grigor'ev, S.V., and Haramus, V., Evolution of composition and fractal structure of hydrous zirconia xerogels

during thermal annealing, *Russ. J. Inorg. Chem.*, 2010, vol. 55, pp. 155–161.

48. Simonenko, E.P., Simonenko, N.P., Kopitsa, G.P., Almasy, L., Gorobtsov, F.Yu., Sevast'yanov, V.G., and Kuznetsov, N.T., Heat-treatment-induced evolution of the mesostructure of finely divided $Y_3Al_5O_{12}$ produced by the sol-gel method, *Russ. J. Inorg. Chem.*, 2018, vol. 63, pp. 691–699.
49. Simonenko, E.P., Simonenko, N.P., Kopitsa, G.P., Mokrushin, A.S., Khamova, T.V., Sizova, S.V., Tsvigun, N.V., Pipich, V., Gorshkova, Y.E., Sevastyanov, V.G., and Kuznetsov, N.T., A sol-gel synthesis and gas-sensing properties of finely dispersed $ZrTiO_4$, *Mater. Chem. Phys.*, 2019, vol. 225, pp. 347–357.
50. Averin, I.A., Karmanov, A.A., Moshnikov, V.A., Pronin, I.A., Igoshina, S.E., Sigaev, A.P., and Terukov, E.I., Correlations in infrared spectra of nanostructures based on mixed oxides, *Phys. Solid. State*, 2015, vol. 57, pp. 2373–2381.
51. Tsai, M.T., Effects of hydrolysis processing on the character of forsterite gel fibers. Part I: Preparation, spinnability and molecular structure, *J. Eur. Ceram. Soc.*, 2002, vol. 22, no. 7, pp. 1073–1083.
52. Niznansky, D. and Rehspringer, J.L., Infrared study of SiO_2 sol to gel evolution and gel aging, *J. Non-Cryst. Solids*, 1995, vol. 180, nos. 2–3, pp. 191–196.
53. Wang, S.-T., Chen, M.-L., and Feng, Yu-Qi, A meso-macroporous borosilicate monolith prepared by a sol-gel method, *Microporous Mesoporous Mater.*, 2012, vol. 151, pp. 250–254.
54. Zha, C., Atkins, G.R., and Masters, A.F., Preparation and spectroscopy of anhydrous borosilicate sols and their application to thin films, *J. Non-Cryst. Solids*, 1998, vol. 242, pp. 63–67.
55. Kaşgöz, A., Misono, T., and Abe, Y., Sol-gel preparation of borosilicates, *J. Non-Cryst. Solids*, 1999, vol. 243, pp. 3168–3174.
56. Levitski, I.A. and Gailevich, S., Influence of divalent cations on the process of phase separation in borosilicate glasses, *Vest. Nats. Akad. Nauk Belarusi*, *Ser. Khim. Nauk*, 2003, no. 3, pp. 111–116.
57. Lee, Y.-Y., Ho, W.-J., Syu, J.-K., Lai, Q.-R., and Yu, C.-M., 7.9% efficiency silicon solar cells by using spin-on films processes, in *PIERS Proceedings*, *2011*, *Suzhou*, *China*.
58. Dominguez, M.A., Luna-Lopez, J.A., Moreno, M., Orduna, A., Garcia, M., Alcantara, S., and Soto, S., Solution-processed transparent dielectric based on spin-on glass for electronic devices, *Rev. Mex. Fis.*, 2016, vol. 62, pp. 282–284.
59. Das, A., Development of high-efficiency boron diffused silicon solar cells, *PhD Dissertation*, Georgia Inst. Technol., 2012.
60. Zeng, K., Wallace, J.S., Heimburger, C., Sasaki, K., Kuramata, A., Masui, T., Gardella, J.A., and Singisetti, U., Ga_2O_3 MOSFETs using spin-on-glass source/drain doping technology, *IEEE Electron Device Lett.*, 2017, vol. 38, no. 4, pp. 513–516.
61. Singha, B. and Solanki, C.S., Boron-rich layer properties formed by boron spin on dopant diffusion in n-type silicon, *Mater. Sci. Semicond. Proc.*, 2017, vol. 57, pp. 83–89.
62. Yang, N., Li, S., Yang, J., Li, H., Ye, X., Liu, C., and Yuan, X., Avoidance of boron rich layer formation in the industrial boron spin-on dopant diffused n-type silicon solar cell without additional oxidation process, *J. Mater. Sci.: Mater. Electron.*, 2018, vol. 29, pp. 20081–20086.